

高能激光短距离传输光束质量测量仿真与实验研究

李 杨¹, 刘 磊^{2,1*}, 王 钢¹, 王文涛¹, 唐晓军¹

(1. 华北光电技术研究所, 北京 100015;
2. 北京理工大学光电学院, 北京 100081)

摘要: 准确测量光束质量对于高能激光系统性能的评估至关重要, 相比传统的远距离传输测量后再修正的方法, 短距离传输后的光束质量更接近激光系统出口处的真实情况。建立激光短距离传输模型, 采用多层相位屏法, 分析空气湍流等因素对激光远场光斑形态和光束质量的影响。结果表明, 在 20 m 的较短传输路径上, 风速、空气相对湿度、功率等影响热晕效应的因素对光束质量影响较小, 常规条件范围内, 光束质量因子 β 值劣化不超过 15%, 而空气湍流效应对高能激光光束质量的影响较明显, 随着空气湍流强度 C_n^2 由 $1 \times 10^{-18} \text{ m}^{-2/3}$ 增大到 $1 \times 10^{-12} \text{ m}^{-2/3}$, β 值从 1.0848 增大至 8.9933; 湍流强度对不同口径激光光束的光束质量影响也不尽相同, 口径越大, 受湍流强度影响越大。文中搭建实物光路, 使用 700 mm 口径平行光管进行验证, 在 $C_n^2 < 1 \times 10^{-14} \text{ m}^{-2/3}$ 的情况下, 测得 $\beta = 2.63$, 与模拟结果相符, 实验中还发现, 可以通过搅散空气的方法来减小湍流强度。实验结果表明: 将空气湍流强度控制在 $1 \times 10^{-14} \text{ m}^{-2/3}$ 以下, 光束质量因子不小于 3 的高能激光系统光束质量测量偏差小于 5%, 为大口径激光系统出口光束质量测量提供一种解决方案。

关键词: 高能激光; 光束质量测量; 湍流效应; 热晕效应; 数值模拟

中图分类号: O436

文献标志码: A

DOI: 10.3788/IRLA20240249

0 引言

高能激光被广泛应用于多个领域, 如高能物理、工业、医疗、军事安全等。据公开报道, 迄今为止, 输出功率最高的激光器为 2010 年美国制造的化学激光器, 输出功率高达兆瓦级别, 固体激光器也可实现 100 kW 级别的激光输出^[1-2]。随着高能激光器输出功率、光学口径的增大, 学者也更关注高能激光系统的远场光斑分布形态与光束质量^[3]。对目标处的光场分布与光束质量进行研究, 可以更好地评估高能激光系统的性能。业内有多种激光光束质量的评价指标, 如 M^2 因子、衍射极限倍数 β 因子、桶中功率比 BQ 、斯特列尔比 S_R 等, 都从不同的角度描述了激光光束质量^[4-5]。

激光在空气中传输时, 随着口径和功率的增大, 与空气的相互作用也更明显, 主要体现为湍流作用和

热晕效应。空气湍流属于空气中粒子的随机运动^[6], 其产生需要具备一定的动力学和热力学条件, 太阳辐射、风速剪切、热对流等过程都会造成空气温度和速度场的随机改变, 进一步导致风速的变化, 使得空气密度和气压出现随机变化, 引起粒子的随机运动, 一般用折射率结构常数 C_n^2 描述其强度。热晕效应是一种非线性效应, 发生在高能激光传输到空气的过程中^[7]。激光在空气中传输时, 部分能量被分子、气溶胶等颗粒吸收, 引起折射率的变化, 降低传输到目标上的光强, 也导致热散焦^[8]。学者们很早就开始了对湍流作用、热晕效应的研究, GEBHARDT^[9] 简化了大气模型, 将吸收、散射、湍流等大气效应互相关联。SMITH^[8] 分析热晕效应, 给出光束峰值强度经验公式。HUANG Yinbo 等^[10-11] 对激光传输进行了数值分析, 并建立激光传输中光束扩展与热晕效应、湍流效应的定标关系。ZHANG Jianzhu 等^[12] 引入统计分析

收稿日期: 2024-06-06; 修訂日期: 2024-07-15

作者简介: 李杨, 女, 硕士生, 主要从事激光大气传输与测量方面的研究。

导师简介: 唐晓军, 男, 研究员级高工, 硕士生导师, 硕士, 主要从事固体激光技术、激光大气传输与测量方面的研究。

通讯作者: 刘磊, 男, 研究员级高工, 硕士生导师, 硕士, 主要从事固体激光技术、激光大气传输与测量方面的研究。

模型, 得到大气参数精度对于激光传输精度的影响。LI Xiaoqing 等^[13] 则数值模拟了阵列合成光束的湍流效应、热晕效应, 用多种评价参数介绍了空气湍流、热晕对激光到靶光束质量的影响。目前关于高功率大口径激光传输的仿真与实验, 主要集中在长距离传输上。

高能激光光束质量测量主要分为两种类型^[4]: 一种是在发射出口处布设系统, 用透镜聚焦的方法, 在焦平面处测量光斑, 即远场光斑分布, 计算光束质量, 但由于发射系统口径较大, 发射望远镜调焦范围有限, 在工程上实现比较困难; 另一种则是远距离传输后测量光束质量 β_a , 同时测量大气相干长度, 并扣除大气影响, 计算推出发射出口处的 β 值。由于湍流、热晕的复杂性与随机性, 以及无法实时获取传输光路上每一点的湍流强度、风速、湿度、温度等相关参数, 在大气条件较差的情况下, 修正量远大于光束质量真

$$U(x, y) = \frac{-i}{\lambda} \exp(ikz) \exp\left(ik \frac{x^2 + y^2}{2z}\right) \cdot \iint U_0(x_0, y_0) \times \exp\left(ik \frac{x_0^2 + y_0^2}{2z}\right) \cdot \exp[-i2\pi(f_x x_0 + f_y y_0)] dx_0 dy_0 \quad (2)$$

式中: z 为传输距离; f_x 、 f_y 分别为 x 、 y 方向的空间频率; U 为观察平面光场分布; U_0 为入射光场分布。

考虑光场分布为高斯型的激光光束, 即:

$$U_0(x_0, y_0) = \sqrt{\frac{P}{\pi\omega_0^2}} \exp\left(-\frac{x_0^2 + y_0^2}{\omega_0^2}\right) \quad (3)$$

式中: P 为出射激光功率; ω_0 为光束半径。将 U_0 的表达式代入公式 (2), 即可得到无扰动高斯型激光传输的光场。激光传输过程中考虑空气湍流作用、热晕效应, 均在此基础上进行。

$$U_{z+1} = \exp\left(-\frac{i}{4k}\Delta z \nabla_\perp^2\right) \cdot \exp\left[-\frac{ik}{2} \int_z^{z+\Delta z} \left(\frac{n^2}{n_0^2} - 1\right) dz\right] \cdot \exp\left(-\frac{i}{4k}\Delta z \nabla_\perp^2\right) U_z \quad (4)$$

相位屏可以采用功率谱反演法来生成^[16], 其实现步骤为, 生成一个随机复矩阵 a , 用大气湍流功率谱对其进行滤波, 然后通过逆傅里叶变换, 即可得到由空气扰动造成的相位畸变。文中采用的是 kolmogorov 谱^[17], 即:

$$\Phi_n(\kappa, z) = 0.033 C_n^2(z) \kappa^{-11/3} \quad (5)$$

式中: κ 为标量波矢; C_n^2 受温度、空气湿度、风速等因素影响明显^[18]。可得到对应相位屏 $\Phi(\vec{r})$ 为:

实值, 误差较大。因此如果需要获得更真实的发射光束质量测量值, 短距离传输后聚焦测量法更优。

1 激光传输基础理论

1.1 惠更斯-菲涅尔原理

首先考虑激光在无扰动情况下的传输。激光光场由麦克斯韦方程组描述^[14], 近轴近似下, 波动方程可简化为:

$$\nabla_\perp^2 U + 2ik \frac{\partial U}{\partial z} + k^2 \left(\frac{n^2}{n_0^2} - 1\right) U = 0 \quad (1)$$

式中: $\nabla_\perp^2 = \partial^2 / \partial x^2 + \partial^2 / \partial y^2$; U 为光场分布; $k = 2\pi/\lambda$, 为光束波数, λ 为激光波长; n_0 为初始折射率分布; n 为扰动后的折射率分布。

对于无扰动传输, 即 $n_0 = n$, 此时采用惠更斯-菲涅尔原理近似可得到传输后光场为:

$$U(x, y) = \iint a(\vec{k}_r) \sqrt{\Phi_n(\vec{k}_r)} e^{i\vec{r} \cdot \vec{k}_r} d\vec{k}_r \quad (6)$$

1.2 多层相位屏法

在综合考虑空气湍流作用和热晕效应对激光传输的影响时, 多层相位屏法是重要研究方法之一^[15]。其基本原理为: 将激光沿传输方向 z 分为 n 段, 每一段的长度为 Δz , 在每段中点处设置一个相位屏, 则激光在每段 Δz 的传输都可以分成三个步骤: 1) 激光自由传输了 $\Delta z/2$ 距离; 2) 激光受到附加的大气扰动; 3) 激光继续自由传输了 $\Delta z/2$ 距离。 $z=z$ 平面处的光场 U_z 传播一个 Δz 距离达到平面 $z=z+\Delta z$ 处的光场 U_{z+1} 可表示为:

$$\Phi(\vec{r}) = \iint a(\vec{k}_r) \sqrt{\Phi_n(\vec{k}_r)} e^{i\vec{r} \cdot \vec{k}_r} d\vec{k}_r \quad (6)$$

式中: \vec{k}_r 为 \vec{r} 位置处的波数。

热晕主要由 3 个基本方程决定^[14], 分别为激光传输近轴近似的波动方程 (公式 (2))、空气密度变化等效方程^[19] 和标准条件下空气折射率与密度之间的关系式:

$$v_x \frac{\partial \rho_1}{\partial x} = \frac{1-\gamma}{C_s^2} \alpha I_p \quad (7)$$

$$\frac{n^2}{n_0^2} - 1 \approx 2(n_0 - 1) \frac{\rho_1}{\rho_0} \quad (8)$$

式中: γ 为比热容比; C_s 为声速; I_p 为激光光强; ρ_0 为空气初始密度; ρ_1 为空气扰动密度。根据该方程即可求解出热晕效应。

将空气湍流作用、热晕效率综合考虑, 即为公式(4)中的空气扰动项。

1.3 透镜聚焦传输

在考虑光场短距离传输后, 需要进一步通过透镜会聚, 使其成像在焦平面处^[20], 才可得到所需远场光斑信息。考虑无限大的无像差薄透镜, 光波从透镜传输 f 距离, 到达焦平面的光场复振幅可表示为:

$$U_f(x_f, y_f) = \frac{1}{i\lambda f} \exp \left[i \frac{k}{2f} (x_f^2 + y_f^2) \right] \cdot \mathcal{F} \left\{ U(x', y') \exp \left[-i \frac{k(x^2 + y^2)}{2f} \right] \right\} \quad (9)$$

式中: U_f 为焦平面上复振幅分布; f 为透镜焦距, 焦平面上的光场即为短距离传输后得到的远场光场。

1.4 衍射极限倍数 β 因子

高能激光的光束质量一般采用 β 因子^[4] 衡量:

$$\beta = \frac{dD}{2.44f\lambda} \quad (10)$$

式中: d 为环围功率为总功率 84% 时的光斑直径; D 为发射系统通光孔径; β 因子综合考虑了激光能量传递中影响光束质量的各个因素, 更适用于评价高能激光系统光束质量。

2 激光短距离传输模型

高功率大口径激光系统出口处的光束质量短距测量光路如图 1 所示, 激光从出口发出后, 短距离传输到达分束镜, 99% 以上的光被反射至功率计, 仅剩不足 1% 的光通过分光透镜, 再经过缩束聚焦系统汇

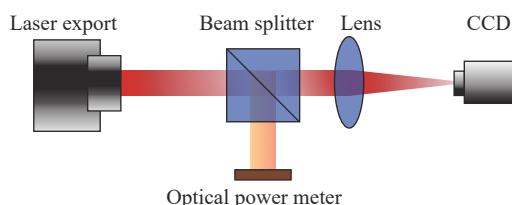


图 1 激光出口处光束质量短距测量光路示意图

Fig.1 Schematic diagram of beam quality short-range measurement at the laser system export

聚后, 成像在 CCD(Charge Coupled Device) 上, 通过分析 CCD 获取的光斑分布图, 就可计算得到所需的光束质量等信息。根据图 1 光路图建立仿真模型。高斯型激光准直输出, 经过多个空气相位屏, 经透镜调制、聚焦后, 在焦平面处成像, 得到远场光斑分布, 测量光斑分布, 并计算其 β 因子。

3 计算结果与讨论

3.1 空气湍流强度、横向风速和空气相对湿度对光束质量的影响

以实际高功率大口径激光系统为例进行计算。假设出射激光波长 $\lambda = 1064 \text{ nm}$, 传输距离 $z = 20 \text{ m}$, 折射率初始值 $n_0 = 1.00029$, 进行短距离传输模拟, 并计算对应的 β 值。

如图 2 所示, 分别为高能激光在不同强度湍流中短距离传输的远场光斑图。采用横向风速 $v = 5 \text{ m/s}$, 空气相对湿度 $RH = 90\%$, 光束直径 $D = 700 \text{ mm}$, 光束功率 $P = 20 \text{ kW}$, 根据 Davis 对湍流强度的划分, 湍流可分为强湍流: $C_n^2 > 2.5 \times 10^{-13} \text{ m}^{-2/3}$ 、中等湍流:

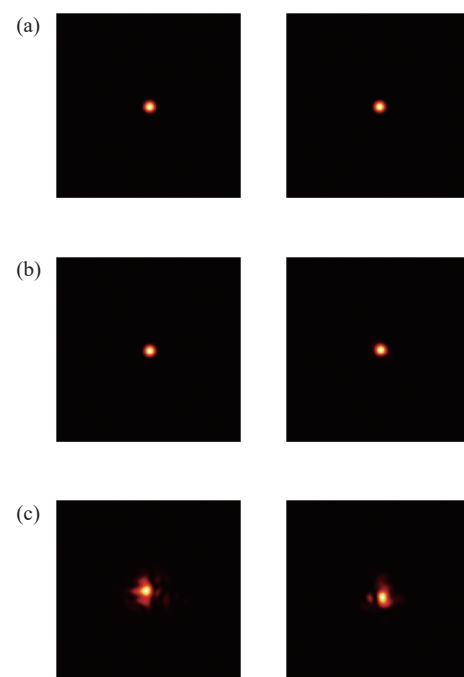


图 2 (a) 弱湍流下的远场光斑图; (b) 中等湍流下的远场光斑图; (c) 强湍流下的远场光斑图

Fig.2 (a) Far-field light spots under weak turbulence; (b) Far-field light spots under moderate turbulence; (c) Far-field light spots under strong turbulence

$6.4 \times 10^{-17} \text{ m}^{-2/3} < C_n^2 < 2.5 \times 10^{-13} \text{ m}^{-2/3}$ 和弱湍流: $C_n^2 < 6.4 \times 10^{-17} \text{ m}^{-2/3}$ 。弱湍流情况下光斑基本没有变化, 强湍流时光斑畸变严重, 甚至出现旁瓣, 但并未呈现出典型的热晕的形态。由于添加了横向风, 光斑在横向方向上有一定程度扩展。图 3(a)给出了 β 因子关于 C_n^2 的曲线, 由图 3(a)可知, β 因子主要受 C_n^2 影响, 随着 C_n^2 的增大, β 值从 1.1806 增大至 8.6967, 与远场光斑反映出的信息一致, 当 $C_n^2 < 10^{-13} \text{ m}^{-2/3}$ 时, β 值小于 2.67。图 3(b)给出了计算 100 次相同激光经过随机生成给定强度区间内 C_n^2 时的 β 值波动。弱湍流中 β 值波动很小, 数值稳定在 1.23 附近, 中等湍流情况下 β 值位于 1.24~3.81 之间, 强湍流中 β 值在 3.08~10.08 之间大幅波动。随着 C_n^2 的增大, β 计算值的方差也进一步增大, 分别为 0.0008、0.1263、1.0921, 进一步说明了高强度的湍流对于激光传输的影响更严重。

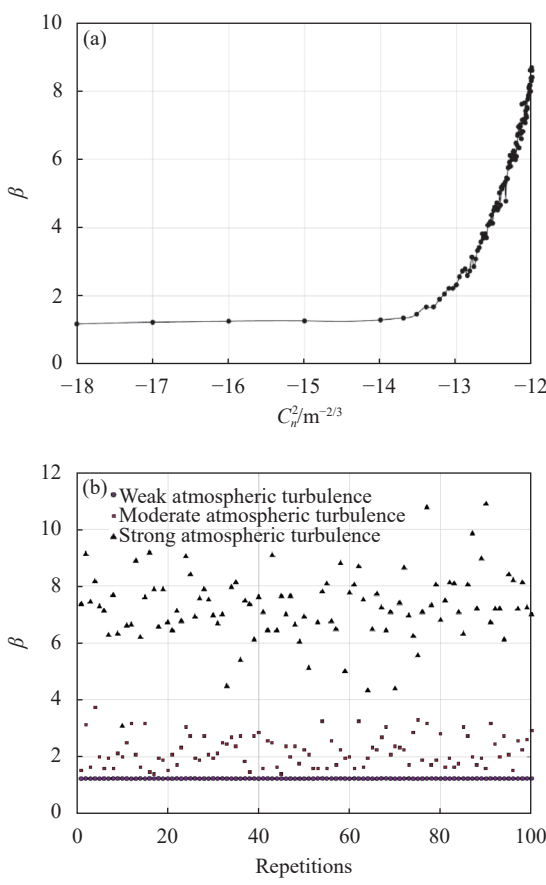


图 3 (a) C_n^2 对 β 值的影响曲线; (b) 不同 C_n^2 下的 β 值

Fig.3 (a) C_n^2 influence curve on β factors; (b) β factors under different C_n^2

除了空气湍流强度, 文中还讨论了其他因素对于

β 值的影响。图 4(a)给出了不同风速对 β 值的影响, 对于不同速度的横向风, β 值相差在 10% 以内, 在弱湍流、中等湍流强度情况下, 相差不超过 3%。图 4(b)给出了不同相对湿度对 β 值的影响, 对于不同空气相对湿度, 对应不同的吸收系数, β 值相差不超过 15%, 且弱湍流、中等湍流区间内, 相差在 2% 以内。

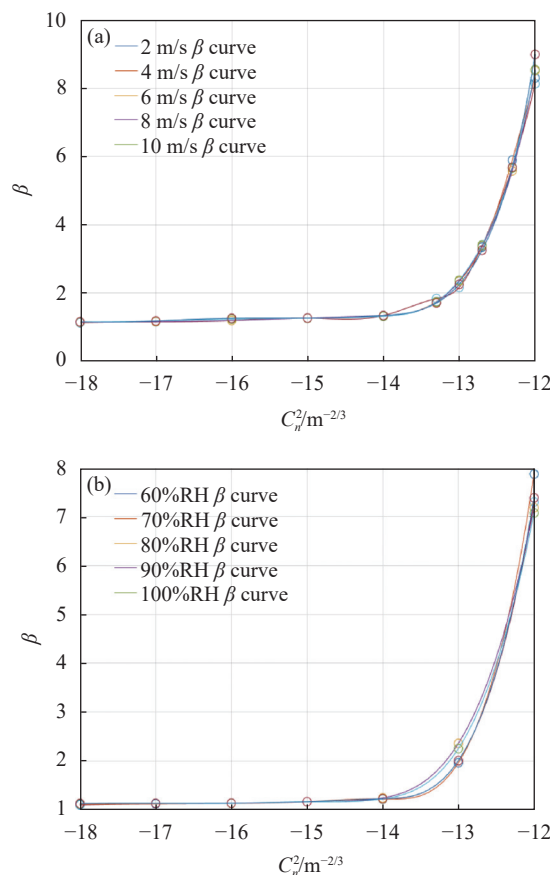


图 4 (a) 横向风速对 β 因子值的影响曲线; (b) 相对空气湿度对 β 因子值的影响曲线

Fig.4 (a) Influence curves of transverse wind speed on β factor; (b) Influence curves of relative air humidity on β factor

3.2 光束直径、光束功率、初始 β 因子对光束质量的影响

除了传输光路上不同因素的影响, 文中还讨论了光束自身性质对于 β 值的影响。图 5(a)给出了不同光束直径对 β 值的影响, β 值随着 ω_0 的增大而增大, 在 $C_n^2 \leq 10^{-14} \text{ m}^{-2/3}$ 的情况下, 不同直径的 β 值相差约为 15%, 当 C_n^2 达到强湍流时, 不同直径的 β 值相差高达 80%。因此对于大口径激光光束质量测量来说, 应该

尽可能的降低湍流强度。图5(b)则给出了不同光束功率P对 β 值的影响,对于不同的功率P, β 值计算误差值在2%以内,即短距传输中激光功率的影响非常小,因此可以使用低功率激光模拟高功率激光进行短距离传输实验。

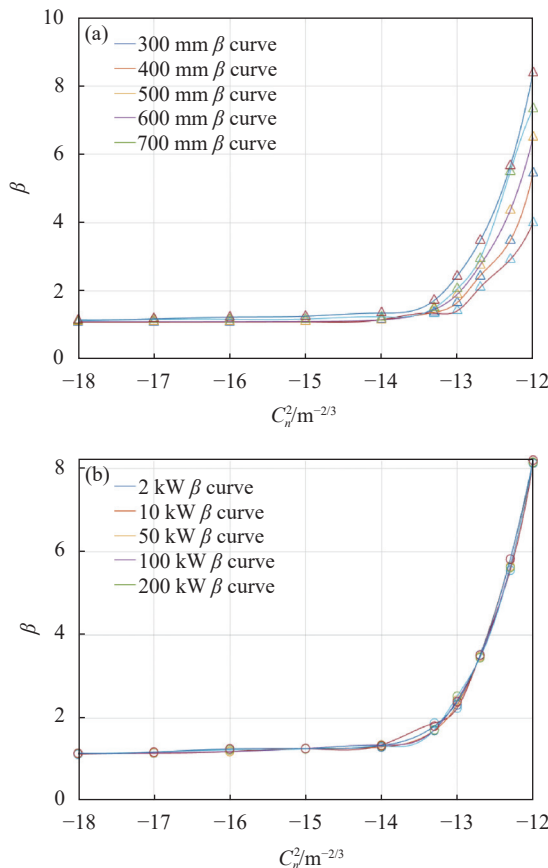


图5 (a) 光束口径对 β 因子值的影响曲线;(b)出射光功率对 β 因子值的影响曲线

Fig.5 (a) Influence curves of beam diameter on β factor; (b) Influence curves of outgoing light power on β factor

图6给出了初始 β 值不同的激光传输后 C_n^2 对 β 值的影响,当 $C_n^2 \leq 10^{-14} \text{ m}^{-2/3}$ 时, β 值与初始 β 值相差不超过5%,初始 β 值 >4 时甚至会出现传输后 β 值优于初始 β 值的情况。随着 C_n^2 从 $10^{-18} \text{ m}^{-2/3}$ 增大至 $10^{-12} \text{ m}^{-2/3}$,初始 β 值=1时, β 值劣化高达840%,而初始 β 值=6时,劣化仅为174%。结果表明,短距离传输后的光束质量不仅受传输光路影响,也与激光系统出口的光束质量直接相关,特别是测量环境满足 $C_n^2 \leq 10^{-14} \text{ m}^{-2/3}$ 时,此时测量的 β 值主要受激光系统出口处 β 值的影响。

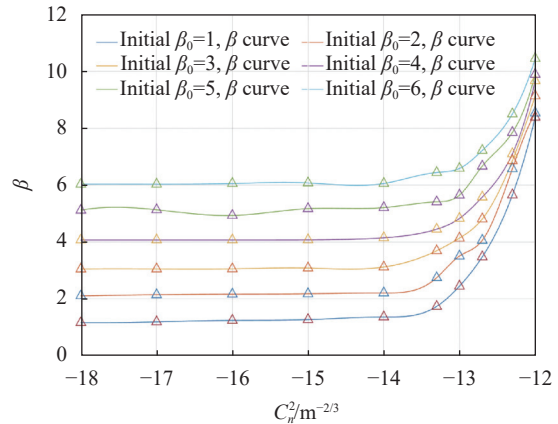


图6 不同初始 β 值下的 C_n^2 对 β 值的影响曲线

Fig.6 The impact curve of C_n^2 on β factor under different initial β factors

3.3 传输距离对光束质量的影响

考虑中等强度湍流区间内不同传输距离的 C_n^2 对 β 值的影响。如图7所示,传输距离为2 m时, β 值几乎没有变化,数值在1.4以下,而当传输距离到达20 m后, β 值随 C_n^2 增大而近似呈线性关系增大。而当 $C_n^2 \leq 10^{-14} \text{ m}^{-2/3}$ 时,20 m传输距离内, β 值偏差在8%内,这进一步说明了,高功率大口径激光短距离传输,仍不可忽略传输光路上的空气湍流影响。

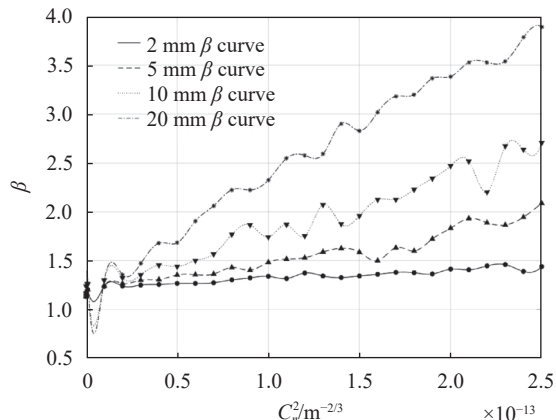


图7 不同传输距离下 C_n^2 对 β 值的影响曲线

Fig.7 Influence curves of C_n^2 on β factors at different transmission distances

3.4 小结

表1给出了不同影响因素对于 β 值的影响汇总。

表 1 不同影响因素对 β 值的影响大小Tab.1 The magnitude of the effect of different influences on β factor

C_n^2	Enormous influence
Transverse wind speed	Almost no effect
Relative air humidity	Almost no effect
Beam diameter	Certain implications
Outgoing laser power	Almost no effect
Initial β factor	Certain implications
Transmission distances	Certain implications

4 实验验证

采用大口径平行光管模拟大口径激光系统进行短距离传输实验,如图 8 所示,采用平行光管通光直径 $D = 700 \text{ mm}$, $f = 30 \text{ m}$, 进行实验。如图 9 所示,在 C_n^2 为 $10^{-16} \text{ m}^{-2/3}$ 量级时, β 值为 1.2333, 在 C_n^2 为 $10^{-15} \text{ m}^{-2/3}$ 量级时, β 值为 2.6333, 与理论值相近。



图 8 700 mm 平行光管图

Fig.8 700 mm parallel light tube

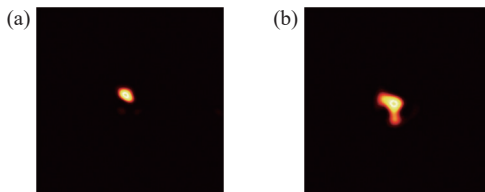
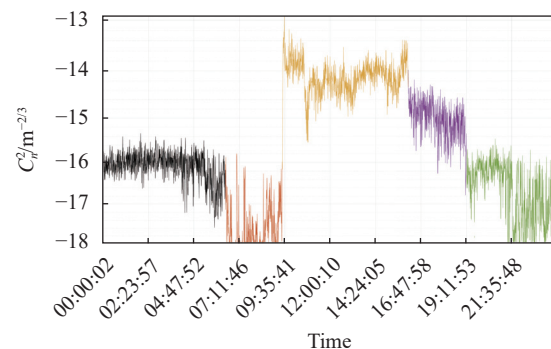


图 9 (a) 700 mm 平行光管弱湍流远场光斑图; (b) 700 mm 平行光管中等湍流远场光斑图

Fig.9 (a) Light spot of weak turbulence far field in 700 mm parallel light tube; (b) Light spot of moderate turbulence far field in 700 mm parallel light tube

在测量光束质量时, 使用温度脉动仪, 采集了空气湍流强度数据。如图 10 所示, 密闭室内 00:00—

06:30 静置, 即没有任何人员活动, 此时由于室内温度较低且整体分布均匀, $C_n^2 < 3 \times 10^{-16} \text{ m}^{-2/3}$, 为中等湍流强度; 在 07:30 日出附近 2 h 内处于一日内温度最低时间段, 达到了弱湍流强度; 09:30—16:00 室内有人员活动, 增强了室内空气运动, 同时由于太阳辐射的加热作用, 引起室内温度变化, $C_n^2 > 10^{-13} \text{ m}^{-2/3}$, 此时不宜进行光束质量测量; 16:05 后打开室内风扇搅散空气, 破坏了室内温度分层, 湍流强度逐步下降, 1 h 后稳定至 $5 \times 10^{-15} \text{ m}^{-2/3}$; 19:30 日落后时间段, 再次静置, 室内温度也逐渐下降, 湍流强度逐步下降, 但仍有一定程度的波动, 在弱湍流、中等湍流区间内波动。

图 10 室内不同时间段 C_n^2 的变化Fig.10 Indoor changes of C_n^2 in different time periods

采用静置或搅散空气的方式, 均在一定程度上可以使 C_n^2 下降至对光束质量影响较小的强度。搅散空气一定程度上破坏了热对流等产生湍流的过程, 在实验中, 比静置更具有实用价值, 同时测量光束质量需要避免急剧升温、降温时间段。在搅散空气可达到的湍流强度条件下, 激光传输产生的相位畸变较小。此时测量的光束质量, 受到传输光路的影响较小, 可近似用来反映激光系统出口处的情况。

5 结 论

文中介绍了高功率大口径激光光束质量测量的研究进展。建立高功率大口径激光短距离传输模型, 分别讨论了短距离内空气湍流、热晕效应对激光传输的影响。短距离传输后, 常规条件范围内, β 值劣化不超过 15%, 而空气湍流效应对高能激光光束质量的影响较明显。不同口径的光束所受影响也存在差异, 口

径越大,湍流强度较大, β 值劣化越大。对于不同强度的湍流, β 值的计算值也存在不同范围的波动,在中等湍流、弱湍流的情况下,测量结果相近。20 m 传输距离内,满足 $C_n^2 \leq 10^{-14} \text{ m}^{-2/3}$ 时, β 值偏差在 8% 内。不同初始 β 值的激光经传输后,光束质量劣化情况也不同,初始光束质量越优秀,劣化越严重。并搭建实物光路进行验证, $C_n^2 < 10^{-14} \text{ m}^{-2/3}$, β 值不超过 2.67,而搅散空气可将空气湍流强度降至该区间内,为大口径激光系统出口光束质量测量提供一种解决方案。

高能激光短距离传输并聚焦测量光束质量所得到的数值更接近激光系统出口处的光束质量,更适用于评价激光系统性能的优劣。但实际测量中,仍需要考虑从激光系统出口至分束镜处的这段距离内的空气的扰动,并尽可能减小其对所获光斑分布、光束质量的影响。文中简化了光路,并未考虑实际存在的光路交叠部分的情况,同时,文中只讨论了开放空间高功率大口径激光的传输影响,光束系统内激光传输所受的影响还需要进一步分析完善。

参考文献:

- [1] LIU Lihui, TAN Bitao, ZHANG Xueyang, et al. The airborne laser project in the united states[J]. *Laser & Infrared*, 2019. (in Chinese)
- [2] XU Xiaojun. Development and challenges of high energy diode pumped alkali lasers (*invited*) [J]. *Laser & Optoelectronics Progress*, 2024, 61(1): 0114002. (in Chinese)
- [3] LIU Zejin, YANG Weiqiang, HAN Kai, et al. Research on the design criteria of laser weapons [J]. *Chinese Journal of Lasers*, 2021, 48(12): 1201001. (in Chinese)
- [4] CHEN Shangwu. Study of problems related to beam quality evaluation of high-energy laser systems[D]. Hangzhou: Zhejiang University, 2007. (in Chinese)
- [5] WANG Yunping, HUANG Jianyu, QIAO Guanglin. A method for evaluating high energy laser beam quality [J]. *Journal of Optoelectronics-Laser*, 2001, 12(10): 1029-1033. (in Chinese)
- [6] CHEN Chunyi, YANG Huamin. Correlation between turbulence impacted optical signals collected via a pair of adjacent spatial-mode receivers [J]. *Optics Express*, 2020, 28(10): 14280-14299.
- [7] WANG S C H, PLONUS M A. Optical beam propagation for a partially coherent source in the turbulent atmosphere [J]. *Journal of the Optical Society of America*, 1979, 69(9): 1207-1304.
- [8] SMITH D C. High-power laser propagation: thermal blooming [J]. *Proceedings of the IEEE*, 1977, 65(12): 1679-1714.
- [9] GEBHARDT F G. High power laser propagation [J]. *Applied Optics*, 1976, 15(6): 1479-1493.
- [10] HUANG Yinbo, WANG Yingjian. Numerical analysis of the scaling laws about focused beam spreading induced by the atmosphere [J]. *Acta Physica Sinica*, 2006, 55(12): 6715-6719. (in Chinese)
- [11] HUANG Yinbo, WANG Yingjian. Effect of the measurement errors of atmospheric parameters on the laser propagation effects [J]. *High Power Laser and Particle Beams*, 2006, 18(5): 720-724. (in Chinese)
- [12] ZHANG Jianzhu, ZHANG Feizhou. Effect of precision of atmospheric parameters on beforehand-estimation of laser propagation [J]. *High Power Laser and Particle Beams*, 2011, 23(4): 901-905. (in Chinese)
- [13] LI Xiaoqing, JI Xiaoling. Theoretical research progress on the influence of atmospheric turbulence and thermal blooming on characteristics and beam quality of laser array beams propagating in the atmosphere [J]. *High Power Laser and Particle Beams*, 2023, 35(4): 90-100. (in Chinese)
- [14] CHEN Dongquan, LI Youkuan, XU Xishen, et al. Numerical analysis of the scaling laws about focused beam spreading induced by the atmosphere [J]. *High Power Laser and Particle Beams*, 1993, 5(2): 243-252. (in Chinese)
- [15] ZHANG Huimin, LI Xinyang. Numerical simulation of wavefront phase screen distorted by atmospheric turbulence [J]. *Opto-Electronic Engineering*, 2006, 33(1): 14-19. (in Chinese)
- [16] PANACHEV S. Stochastic Functions and Turbulence[M]. Beijing: Science Press, 1976: 146-193.
- [17] XU Guangyong, WU Jian, YANG Chunping, et al. Simulation and optical scintillation research on Gaussian beam in atmosphere turbulence [J]. *Laser Technology*, 2008, 32(5): 548-550. (in Chinese)
- [18] MA Shengjie, HAO Shiqi, ZHAO Qingsong, et al. Atmospheric turbulence intensity estimation based on deep convolutional neural networks [J]. *Chinese Journal of Lasers*, 2021, 48(4): 0401018. (in Chinese)
- [19] MENG Qijun, YANG Xiaoli, AN Xuee. The theory analysis of atmospheric density change in the thermal blooming due to aerosols [J]. *Laser Journal*, 2006(5): 39-40. (in Chinese)
- [20] LIU Zhiqiang, SONG Qinghe, LIU Chao, et al. Fresnel diffraction calculation with virtual light wave field and its application [J]. *Journal of Applied Optics*, 2018, 39(2): 196-199. (in Chinese)

Simulation and experimental study of beam quality measurement for short distance transmission of high power laser

LI Yang¹, LIU Lei^{2,1*}, WANG Gang¹, WANG Wentao¹, TANG Xiaojun¹

(1. China Electronics Technology Group Eleventh Research Institute, Beijing 100015, China;

2. School of Optoelectronics, Beijing Institute of Technology, Beijing 100081, China)

Abstract:

Objective Accurate measurement of beam quality is crucial to the evaluation of laser performance, and compared with the traditional method of measuring and then correcting after long-distance transmission, the beam quality after short-distance transmission is closer to the real situation at the export of the laser. When high-energy laser propagates in the air, as the power increases, the interaction with the air will also become more obvious, mainly reflected in atmospheric turbulence and thermal blooming effects, which will affect the distortion and expansion of the spot shape, leading to a decrease in beam quality. However, current simulations and experiments on high-power large-caliber laser transmission often involve long-distance transmission to obtain target power. After accounting for the effects of atmospheric turbulence and thermal blooming on the transmission path, they then deduce beam quality information for further evaluation. Due to the complexity and randomness of atmospheric turbulence and thermal blooming, as well as the inability to obtain real-time relevant parameters of each point on the transmission optical path, the deduction amount is much greater than the true value of the beam quality under poor atmospheric conditions, resulting in significant errors. Therefore, measuring beam quality directly at the system export, given the short transmission distance, is less affected by nonlinear effects such as atmospheric turbulence and thermal blooming, and thus produces more accurate results.

Methods Firstly, the theories regarding the atmospheric turbulence effect and thermal blooming effect in short-distance transmission were elaborated. Then, we simplified the optical path diagram for measuring beam quality (Fig.1), and established a model simulation based on this optical path diagram, by changing different environmental factors and conducting simulation experiments. Using a parallel light tube with a diameter of 700 mm, at a distance of 20 m, a Charge Coupled Device (CCD) was used to receive the focused spot and calculate its beam quality. While measuring the beam quality, a temperature pulsation meter was used to collect the indoor turbulence intensity during the experimental process, and methods for reducing turbulence intensity were analyzed.

Results and Discussions In the case of 20 m transmission, the beam quality β factor was severely affected by turbulence intensity C_n^2 , and the spot shape underwent significant distortion and expansion as turbulence increases (Fig.2). Further analysis was conducted on the variance of the β factors under different intensities of turbulence. The variance did not exceed 0.08% under weak turbulence, approximately 12.63% under moderate turbulence, and over 100% under strong turbulence (Fig.3). For lateral winds of different speeds, the difference in β factors was within 10%. For different relative humidity of the air, the difference in β factors did not exceed 15%. For different apertures, β factors increased with the increase of aperture size. In this case, the difference in β factors between different apertures was about 15% (Fig.4). When strong turbulence intensity is reached, the difference in β factors between different apertures could reach up to 80% (Fig.5). For different powers, the error in β factors calculation was within 2%. The beam transmission with different initial β factors was also simulated, and the

beam quality measurement deviation of the laser system was less than 5% for the laser system with the air turbulence control intensity controlled below $1 \times 10^{-14} \text{ m}^{-2/3}$ and the beam quality β factor not less than 3 (Fig.6). Different transmission distance also had an impact on the β factors of laser beam quality. When the β factor measurements are stable in the moderate turbulent intervals for a transmission distance of 2 m, whereas it increases approximately linearly for 20 m (Fig.7). The actual measured beam quality of the 700 mm caliber collimator (Fig.8) was consistent with the simulation results (Fig.9). Collecting indoor turbulence intensity variation maps, both static and stirred air could achieve lower turbulence intensity values (Fig.10), which means that in actual measurement processes, atmospheric turbulence intensity can be reduced by stirring air to obtain more accurate values.

Conclusions This article introduces the research progress of high-power laser beam quality measurement. We separately discussed the effects of atmospheric turbulence and thermal blooming on laser transmission over short distances. After short distance transmission, the atmospheric turbulence effect has a greater impact on beam quality, and as C_n^2 increases, the β factors increases from 1.0848 to 8.9933. The influence of factors such as thermal blooming effect and humidity is minimal. In case of moderate and weak turbulence, the difference in β factors for different lateral wind speeds, relative air humidity, and power is within 3%. But for different apertures, when reaching $C_n^2 \leq 10^{-14} \text{ m}^{-2/3}$, the difference in β factors for different apertures is about 15%. When strong turbulence intensity is reached, the difference in β factors for different apertures can reach up to 80%. And in actual measurements, it has been verified that stirring air can also reduce atmospheric turbulence to a certain value. Therefore, it is necessary to minimize the disturbance of the air within the distance from the outlet to the beam splitter, making stirring air more practical. The β factors deviation is within 8% when $C_n^2 \leq 10^{-14} \text{ m}^{-2/3}$ at 20 m transmission distance. The beam quality degradation after transmission is different for lasers with different initial factors, and the more excellent the initial beam quality is, the more serious the degradation is. The experimental results of this paper show that the beam quality measurement deviation of the high-power, large-caliber laser system with beam quality β factor not less than 3 is less than 5% by controlling the air turbulence control intensity below $C_n^2 < 10^{-14} \text{ m}^{-2/3}$, which provides a solution for the beam quality measurement of large-caliber laser export.

Key words: high power laser; beam quality measurement; turbulence effect; thermal blooming effect; numerical simulation